

Essential role of catalyst in vapor-liquid-solid growth of compounds

Masaru Suzuki,^{1,*} Yoshiki Hidaka,¹ Takeshi Yanagida,² Annop Klamchuen,² Masaki Kanai,² Tomoji Kawai,² and Shoichi Kai¹

¹*Department of Applied Quantum Physics and Nuclear Engineering, Kyushu University, 744 Motoooka, Nishi-ku, Fukuoka 819-0395, Japan*

²*The Institute of Scientific and Industrial Research, Osaka University, Mihogaoka 8-1, Ibaraki, Osaka 567-0047, Japan*

(Received 25 January 2011; published 28 June 2011)

The mechanism of the solidification of compound materials, such as oxide crystals, in a vapor-liquid-solid (VLS) system is investigated by model molecular dynamics simulation. A simple model for the VLS growth of a compound crystal is proposed to clarify the general mechanism of how a liquid solvent catalyzes the growth rate. We find that the nucleation process at the solid surface is responsible for limiting the growth rate, and that the solvent catalyzes the nucleation by reducing the critical nucleation size at the liquid-solid interface. Our theoretical suggestion that the ratio of the vapor-solid (VS) growth rate to the VLS growth rate strongly depends on the supply rate qualitatively agrees well with the experimental result. Finally, we simulate the entire process of VLS nanowire formation.

DOI: [10.1103/PhysRevE.83.061606](https://doi.org/10.1103/PhysRevE.83.061606)

PACS number(s): 81.10.Aj, 81.07.Gf, 83.10.Rs

I. INTRODUCTION

Since the vapor-liquid-solid (VLS) processing technique was introduced in the '60s [1], it has been widely applied to building inorganic nanostructures, particularly size-controlled nanowires, made of single-component crystals, such as Si [1–3] and Ge [4,5], and also of metal-oxides including MgO, SnO₂, NiO, and ZnO [6–9]. In the VLS growth, a nanowire is formed controlled by the size and position of the metal droplet, which efficiently captures the material supplied from the vapor phase. Thus, the key mechanism of nanowire structure formation should be the catalytic effect of the solvent liquid on the solidification rate, or in other words, the VLS growth proceeds much faster than vapor-solid (VS) growth under the same material supply condition. In the preceding article [10], we reported an experimental result of SnO₂ growth, suggesting that the VS/VLS growth-rate ratio depends on the material supply rate, and that the VS growth rate can be suppressed at a low supersaturation of supplied oxygen. If such a phenomenon is universal for various oxide materials, understanding this mechanism may provide a theoretical principle for constructing a well-defined nanowire. In this study, we develop a simple model of VLS compound crystal growth in order to determine the general mechanism of the catalytic effect of the solvent. First, a series of solid growth simulations using VLS and VS systems with simple layered configurations (see Fig. 1) are performed to determine the mechanism difference between the two systems. Subsequently, a simulation reproducing the entire process of nanowire growth is performed.

II. MODEL

The simulation system consists of three types of particles, namely, those of the solid growth compound (named A₁ and A₂ particles) and those of the solvent liquid (B particles). Particles interact with each other through the Lennard-Jones (L-J) interactions [11], except the interactions between A₁-A₁ and A₂-A₂ pairs. We independently set values for the interaction

strengths of an A₁-A₂ pair ε_A , a B-B pair ε_B , and an A₁-B (or A₂-B) pair ε_{AB} , as well as for the contact lengths of those pairs, σ_A , σ_B , and $\sigma_{AB} = (\sigma_A + \sigma_B)/2$, respectively. For the interactions between A₁-A₁ and A₂-A₂ pairs, we introduce a new repulsive potential,

$$\phi_{\text{rep}}(r) = 4\varepsilon_A[(\sigma_A/r)^{12} + (\sigma_A/r)^6 + c(r)]. \quad (1)$$

The last term, $c(r)$, indicates the correction at the cutoff length R_{cf} . The cutoff lengths for all the interacting pairs are set to be $R_{cf} = 3\sigma$. With these potentials, A₁ and A₂ particles form a rock-salt-type crystalline compound as the ground-state structure.

The size of the simulation box is $L \times L \times \alpha L$, where αL is the system height (set $\alpha = 1.8$ in this article). Initially, an eight-layer-thick solid substrate consisting of A₁ and A₂ particles with rock-salt order is fixed on the bottom wall. The (0,0,1) surface of the substrate is perpendicular to the bottom wall. The typical system size we use is $L = 32a$, where a is the lattice constant of the rock-salt unit lattice in the equilibrium state. Above the substrate, a flat layer of B-particle solvent is placed in the simulation of the VLS process, while no solvent is added to the VS process (Fig. 1). The side walls have a periodic boundary condition. The temperature of the system is controlled on the top and bottom walls. On the top wall, a particle bath for A₁ and A₂ particles is attached. When the density of the particle bath is set to be ρ^{sup} , new particles are constantly supplied from outside the top wall at the rate $j^{\text{sup}} = \rho^{\text{sup}}\sqrt{2k_B T/\pi}$ per unit area, and all the particles that collide with the top wall from inside the box are removed. The particle bath densities of A₁ particles $\rho_{A_1}^{\text{sup}}$ and of A₂ particles $\rho_{A_2}^{\text{sup}}$ are set independently.

In the following, we use the physical quantities reduced by ε_A , σ_A , and the particle mass m . Thus, time is scaled by $\sqrt{m/\varepsilon_A}\sigma_A$. We denote the reduced temperature $k_B T/\varepsilon_A$ simply as T .

III. RESULTS

We perform a series of simulations using the parameters $\varepsilon_B = 0.18$, $\varepsilon_{AB} = 0.115$, $\sigma_B = 1.59$, and $T = 0.12$. For each simulation, the system is developed without supplying new

*suzuki@athena.ap.kyushu-u.ac.jp

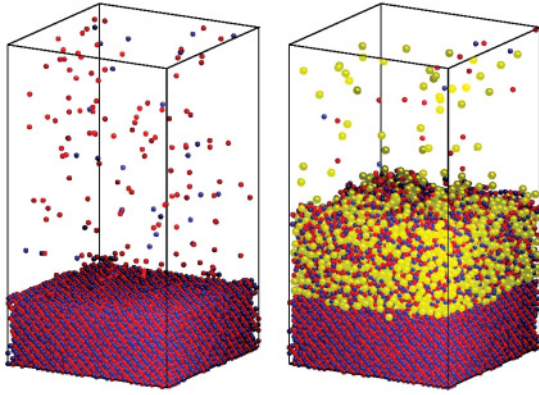


FIG. 1. (Color online) Snapshots during solid growth in VS (left) and VLS (right) systems.

particles until it reaches an equilibrium state (up to $t = 16000$). When the new A_1 and A_2 particles are supplied continuously at $t > 16000$ with the supply densities ρ_{A1}^{sup} and ρ_{A2}^{sup} , respectively, the solid begins to grow. Figure 2 shows the long-time average of solid growth rate (increasing number of particles belonging to the solid per unit area) depending on ρ_{A1}^{sup} in the VS and VLS systems, while the supply density of A_2 is fixed at $\rho_{A2}^{\text{sup}} = 2 \times 10^{-4}$. A finite growth rate in the VLS system is observed even at a relatively low supply density (around $\rho_{A1}^{\text{sup}} \simeq 5 \times 10^{-5}$), whereas the solid in the VS system hardly grows until the supply density reaches $\rho_{A1}^{\text{sup}} \simeq 8 \times 10^{-4}$.

To understand how this strongly nonlinear response of the growth rate to the supply rate occurs, detailed observations during the solid growth are performed. We find that the solid growth at the surface layer is triggered by the formation of a small nuclear cluster. Figure 3 shows the time-dependent solid growth rate and also the area fraction of the solid cluster at each growing layer. Once a small cluster is formed at the surface layer, the solid growth intensely proceeds until the layer is filled up. However, subsequently, there exists a time interval where the solid hardly grows until the nucleation at the next layer occurs.

The reduced nucleation rate on the solid substrate j^{nu} is generally defined as $j^{\text{nu}} = 1/(S\langle\tau\rangle)$ with the area of the

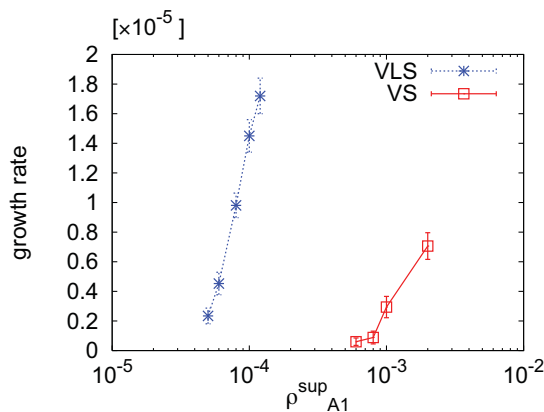


FIG. 2. (Color online) Growth rate of the solid depending on the supply density of A_1 particles ρ_{A1}^{sup} . The supply density of A_2 particles is fixed at $\rho_{A2}^{\text{sup}} = 2 \times 10^{-4}$.

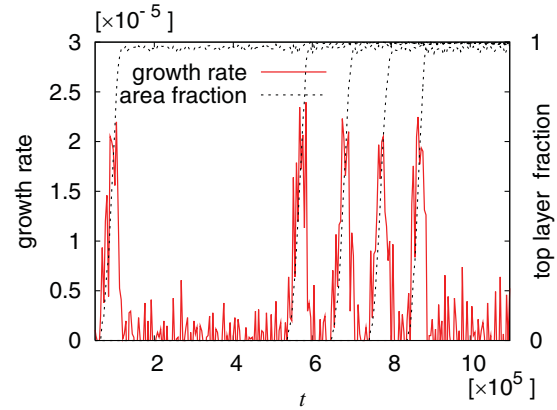


FIG. 3. (Color online) Time evolution of growth rate and area fraction of solid cluster at each surface layer. The result in the VS system with $\rho_{A1}^{\text{sup}} = 1.0 \times 10^{-3}$ is shown as an example.

substrate, S (reduced by σ_A^2), and the expectation value of the waiting time, $\langle\tau\rangle$ (reduced by $\sqrt{m/\epsilon_A\sigma_A}$). In our case, the waiting time for the critical nucleation in the l th layer depends on the area of the layer below it, namely, S_{l-1} , which grows with time. Although the timescale of the cluster growth to fill a layer is much shorter than the typical waiting time τ , still it's not negligible to estimate the nucleation rate accurately, i.e., $S_{l-1}(t)$ cannot be regarded as a step function (see the dashed curves in Fig. 3). Thus, we define the nucleation rate, instead of $j^{\text{nu}} = 1/(S\langle\tau\rangle)$, as

$$j^{\text{nu}} = \frac{1}{\langle \int_{-\infty}^{t_l} S_{l-1}(t) dt \rangle_{t_l}}, \quad (2)$$

where t_l is the time when the critical nucleation at the l th layer occurs. The nucleation rate j^{nu} values estimated using Eq. (2) are shown in Fig. 4. These values show the supply density dependence that is similar to the growth rate shown in Fig. 2, which suggests that the growth rates in both VS and VLS systems are limited by the nucleation rates at the solid surface.

The estimated value of nucleation rate may be associated with some physical quantities following the framework of the classical nucleation theory. Under the steady condition where the outside of the solid is supersaturated at the

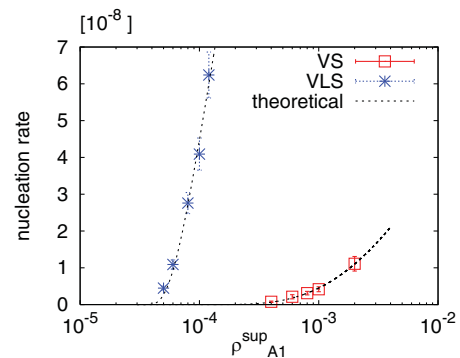


FIG. 4. (Color online) Nucleation rates in the VS and VLS systems depending on the supply density. The points indicate the values estimated by simulation and the dashed curves are the theoretical values.

value of chemical potential $\mu = \mu_{\text{eq}} + \Delta\mu$ and at $\mu = \mu_{\text{eq}}$ (equilibrium condition) inside the solid, the Gibbs free energy gain for forming a two-dimensional nuclear cluster with n particles should be

$$\Delta G(n) = -n\Delta\mu + \gamma\sqrt{n}. \quad (3)$$

The second term on the right-hand side indicates the free energy that is proportional to the boundary length of the nuclear cluster with the proportionality constant γ (two-dimensional surface tension). We denote the reduced chemical potential μ/ε_A simply as μ and $(\sigma_A/\varepsilon_A)\gamma$ as γ . $G(n)$ has a local maximum at

$$n^* = \left(\frac{\gamma}{2\Delta\mu}\right)^2, \quad (4)$$

which is associated with the critical nucleation size. Using the Gibbs free energy gain at the critical size, the nucleation rate is calculated as

$$j^{\text{nu}} = A \exp\left[-\frac{G(n^*)}{T}\right] = A \exp\left(-\frac{\gamma^2}{4\Delta\mu T}\right). \quad (5)$$

Here, A is a dimensionless prefactor independent of $\Delta\mu$. The degree of supersaturation, $\Delta\mu$, in the vapor phase is described with the supply densities ρ_{A1}^{sup} and ρ_{A2}^{sup} under the diluted condition as

$$\Delta\mu = \frac{T}{2} \left[\ln(\rho_{A1}^{\text{sup}}/\rho_v^{\text{eq}}) + \ln(\rho_{A2}^{\text{sup}}/\rho_v^{\text{eq}}) \right]. \quad (6)$$

Here, ρ_v^{eq} is the vapor density of A_1 and A_2 under the equilibrium condition, which is estimated to be $\rho_v^{\text{eq}} = 7.5 \times 10^{-5}$ from the result of preliminary simulations. The nucleation rate values estimated from our simulation result are fitted using Eq. (5) as a function of ρ_{A1}^{sup} via the fitting parameters A and γ , as shown in Fig. 4. The optimal values of these parameters at the vapor-solid interface (in the VS system) and at the liquid-solid interface (in the VLS system) are estimated as

$$\begin{aligned} A_{\text{vs}} &= 1.1 \times 10^{-6}, & \gamma_{\text{vs}} &= 0.75, \\ A_{\text{ls}} &= 4.6 \times 10^{-7}, & \gamma_{\text{ls}} &= 0.29. \end{aligned} \quad (7)$$

The surface tension at the vapor-solid interface, γ_{vs} , is approximately two-and-a-half times larger than that at the liquid-solid interface γ_{ls} , which causes a significant difference in nucleation rate between the VS and VLS systems, as described in Eq. (5). This indicates that the solid growth rate in the VS system at a low supersaturation ($\rho_{A1}^{\text{sup}} \sim 10^{-4}$) is negligibly low because of the large vapor-solid surface tension, or in other words, the solvent can catalyze the solid growth by reducing the surface tension at the liquid-solid interface. The VS/VLS growth rate ratio is described in the following form:

$$j_{\text{vs}}^{\text{nu}}/j_{\text{vls}}^{\text{nu}} \propto \exp\left(\frac{\gamma_{\text{ls}}^2 - \gamma_{\text{vs}}^2}{4\Delta\mu T}\right), \quad (8)$$

which is a monotonically increasing function of $\Delta\mu$, under the condition of $\gamma_{\text{vs}} > \gamma_{\text{ls}}$. This fact includes an important suggestion for constructing a nonowire: Although the nucleation occurs only inside the solvent droplet (VLS growth) at a low supersaturation $\Delta\mu$ that satisfies $j_{\text{vs}}^{\text{nu}}/j_{\text{vls}}^{\text{nu}} \ll 1$, as the ratio $j_{\text{vs}}^{\text{nu}}/j_{\text{vls}}^{\text{nu}}$ increases at a higher supersaturation, the finite growth outside the droplet (VS growth at the substrate surface

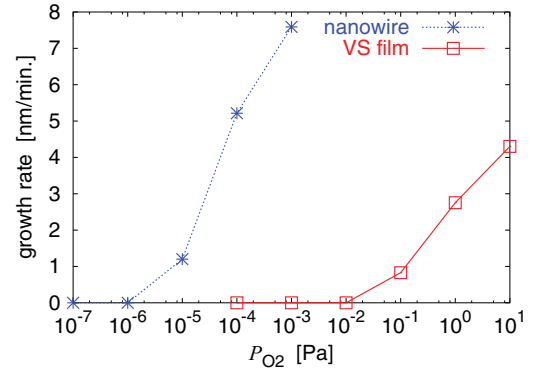


FIG. 5. (Color online) Rates of VLS nanowire growth and VS film growth of SnO_2 depending on the O_2 partial pressure.

and wire sidewalls) would disturb the uniaxial growth of the nanowire.

The simulation result is compared with the experimental data of VLS growth using SnO_2 crystals (details are in Ref. [10]) to verify the above conjecture. Figure 5 shows the growth rate of SnO_2 nanowires using Au solvent droplets (VLS system) and that of SnO_2 films without a solvent (VS system) performed at 700°C . The supply rate of Sn (supplied by laser ablation of the target) is fixed, whereas that of oxygen is varied controlling the partial pressure P_{O_2} . Although the $P_{\text{O}_2} > 10^{-5}$ Pa range is obviously a supersaturation condition because nanowires can grow, the solid hardly grows in the VS system until the partial pressure reaches $P_{\text{O}_2} \simeq 10^{-2}$. This situation is qualitatively similar to the simulation result shown in Fig. 2. Figure 6 shows the diameters of the nanowires at the top and bottom of 500nm axial length. The diameter at the bottom increases with the partial pressure P_{O_2} . This finding indicates that the VS side-wall growth during the VLS axial growth becomes marked as P_{O_2} increases, which is consistent with the discussion around Eq. (8). These experimental results support the theoretical indication that the critical nucleation at the surface limits the growth rate and that the VS growth in the low supersaturation regime is suppressed because of the large surface tension.

Now, we found the condition where the VLS growth rate is much higher than VS growth rate; thus, a wire structure could be formed using our simulation model. We perform

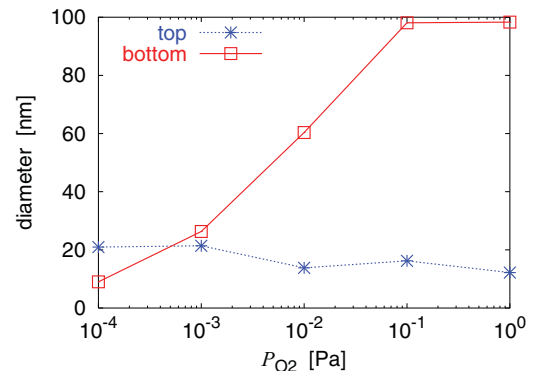


FIG. 6. (Color online) Nanowire diameters at the top and bottom of 500nm SnO_2 nanowires depending on the O_2 partial pressure.

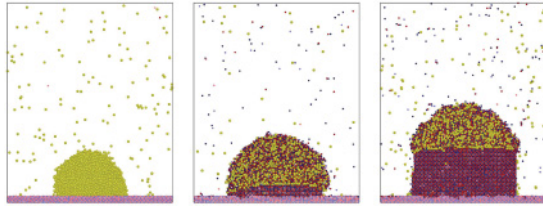


FIG. 7. (Color online) Cross sections during the VLS nanowire growth simulation at $t = 8\,000$ (left), $t = 31\,8000$ (center), and $t = 808\,000$.

a simulation demonstrating the entire process of nanowire construction. The system size is $90a \times 90a \times 108a$, and initially, a droplet consisting of 9000 B particles is set on a four-layer-thick substrate. Figure 7 shows some snapshots during the growth at the supply rates $\rho_{A1}^{\text{sup}} = 1.2 \times 10^{-4}$ and $\rho_{A2}^{\text{sup}} = 5 \times 10^{-4}$ with the same interaction parameters as those considered in the simulations above. The solid growth only proceeds at the liquid-solid surface inside the droplet and a nanowire structure is formed.

IV. SUMMARY AND DISCUSSIONS

In summary, we performed a series of VS and VLS solid-growth simulations using a compound crystal model for the growth material. In both systems, the growth rates are almost limited by the critical nucleation rate at the solid surface. Through the analysis using the nucleation theory, we found that the solvent can catalyze the nucleation in the VLS process by reducing the surface tension of a two-dimensional nuclear cluster formed at the liquid-solid surface. The theoretical suggestions regarding the nonlinear profile of the growth rates and also the growth ratio between both systems ($j_{\text{vs}}/j_{\text{vls}}$) depending on the supply rate were verified by SnO_2 growth experiment.

Though we mainly observed, in our simulation, the mononuclear growth process, in the nanowire growth in real systems, where a large VS interface outside the droplet exists, the polynucleation VS process may become dominant. If a system has so large solid surface area S that the cluster growth

to fill the area S after the nucleation costs longer time (estimated as $\tau_g \sim S/c$ with the reduced cluster growth rate within a layer, c) than the waiting time for a nucleation $\tau \sim 1/(Sj^{\text{nu}})$, polynucleation would be observed. In such cases, the time scale to fill the entire layer can be estimated as (substituting the typical area of the single cluster growth $S_0 \sim \sqrt{c/j^{\text{nu}}}$, which satisfies $\tau_g \sim \tau$, into $\tau_g \sim S_0/c$) $\tau_0 \sim (cj^{\text{nu}})^{-1/2}$. Although this kind of polynucleation provides a little advantage to the VS growth rate, the VLS growth rate inside the droplet can still be faster than that, under the condition with extremely high VLS nucleation rate ($j_{\text{vls}}^{\text{nu}} \gg j_{\text{vs}}^{\text{nu}}$). For example, at the supply rate $\rho_{A1}^{\text{sup}} = 10^{-4}$ and $\rho_{A2}^{\text{sup}} = 2 \times 10^{-4}$, where we measured $j_{\text{vls}}^{\text{nu}} \sim 5 \times 10^{-8}$, $j_{\text{vs}}^{\text{nu}} \sim 2 \times 10^{-13}$ and $c \sim 10^{-1}$, the polynuclear VS layer growth takes much more time, $\tau_{\text{vs}} \sim (cj_{\text{vs}}^{\text{nu}})^{-1/2} \sim 7 \times 10^6$, than the VLS mononucleation, $\tau_{\text{vls}} \sim 1/(S_{\text{vls}}j_{\text{vls}}^{\text{nu}}) \sim 2 \times 10^4$ (with $S_{\text{vls}} \sim 10^3$). In the system with larger droplet, the polynucleation process would occur even in the VLS process, as indicated in Ref. [12].

It should be noted that Eq. (5) is only applicable in the critical nucleation regime where the critical size n^* is larger than unity, which corresponds to $\Delta\mu < \gamma/2$ or $\rho^{\text{sup}} < \rho_v^{\text{eq}} \exp[\gamma/(2T)]$. Above this range of supersaturation, monomers in the vapor phase are easily trapped onto the solid surface. In such cases, the solidification at the solid surface rapidly proceeds and the mass transport toward the surface may limit the growth rate rather than the critical nucleation rate, as reported in Ref. [13]. The complete description of the VLS growth-rate equation including the competitive phenomenon between the mass transport and the surface nucleation would be available through further investigations using our current model.

ACKNOWLEDGMENTS

The authors thank T. Narumi for fruitful discussions. This work was partially supported by the MEXT through a Grant-in-Aid for Scientific Research on Innovative Areas ‘‘Emergence in Chemistry’’ (No. 20111003) and a Grant-in-Aid for Scientific Research (No. 21340110). T.K. was supported by the FIRST program.

-
- [1] R. S. Wagner and W. C. Ellis, *Appl. Phys. Lett.* **4**, 89 (1964).
 - [2] F. M. Ross, J. Tersoff, and M. C. Reuter, *Phys. Rev. Lett.* **95**, 146104 (2005).
 - [3] L. Yu and P. RocaïCabarrocas, *Phys. Rev. B* **80**, 085313 (2009).
 - [4] H. Adhikari, P. C. McIntyre, A. F. Marshall, and C. E. D. Chidsey, *J. Appl. Phys.* **102**, 094311 (2007).
 - [5] D. E. Perea, E. R. Hemesath, E. J. Schwalbach, J. L. Lensch-Falk, and P. W. Voorhees, *Nat. Nanotech.* **4**, 315 (2009).
 - [6] K. Nagashima, T. Yanagida, H. Tanaka, and T. Kawai, *J. Appl. Phys.* **101**, 124304 (2007).
 - [7] A. Marcu, T. Yanagida, K. Nagashima, H. Tanaka, and T. Kawai, *J. Appl. Phys.* **102**, 016102 (2007).
 - [8] T. Yanagida, A. Marcu, H. Matsui, K. Nagashima, K. Oka, K. Yokota, M. Taniguchi, and T. Kawai, *J. Phys. Chem. C* **112**, 18923 (2008).
 - [9] K. Oka, T. Yanagida, K. Nagashima, H. Tanaka, and T. Kawai, *J. Am. Chem. Soc.* **131**, 3434 (2009).
 - [10] A. Klamchuen, T. Yanagida, M. Kanai, K. Nagashima, K. Oka, T. Kawai, M. Suzuki, Y. Hidaka, and S. Kai, *Appl. Phys. Lett.* **97**, 073114 (2010).
 - [11] S. D. Stoddard and J. Ford, *Phys. Rev. A* **8**, 1504 (1973).
 - [12] D. Kashichiev, *Crystal Growth Design* **6**, 1154 (2006).
 - [13] M. Suzuki, Y. Hidaka, T. Yanagida, M. Kanai, T. Kawai, and S. Kai, *Phys. Rev. E* **82**, 011605 (2010).